



HHS Public Access

Author manuscript

Cell Rep. Author manuscript; available in PMC 2020 January 08.

Published in final edited form as:

Cell Rep. 2019 December 24; 29(13): 4608–4619.e4. doi:10.1016/j.celrep.2019.11.110.

Hedgehog Acyltransferase Promotes Uptake of Palmitoyl-CoA across the Endoplasmic Reticulum Membrane

James J. Ascioia^{1,2}, Marilyn D. Resh^{1,2,3,*}

¹Cell Biology Program, Memorial Sloan Kettering Cancer Center, New York, NY, USA

²Biochemistry, Cell Biology and Molecular Biology Graduate Program, Weill-Cornell Graduate School of Medical Sciences, New York, NY, USA

³Lead Contact

SUMMARY

Attachment of palmitate to the N terminus of Sonic hedgehog (Shh) is essential for Shh signaling. Shh palmitoylation is catalyzed on the luminal side of the endoplasmic reticulum (ER) by Hedgehog acyltransferase (Hhat), an ER-resident enzyme. Palmitoyl-coenzyme A (CoA), the palmitate donor, is produced in the cytosol and is not permeable across membrane bilayers. It is not known how palmitoyl-CoA crosses the ER membrane to access the active site of Hhat. Here, we use fluorescent and radiolabeled palmitoyl-CoA probes to demonstrate that Hhat promotes the uptake of palmitoyl-CoA across the ER membrane in microsomes and semi-intact cells. Reconstitution of purified Hhat into liposomes provided further evidence that palmitoyl-CoA uptake activity is an intrinsic property of Hhat. Palmitoyl-CoA uptake was regulated by and could be uncoupled from Hhat enzymatic activity, implying that Hhat serves a dual function as a palmitoyl acyltransferase and a conduit to supply palmitoyl-CoA to the luminal side of the ER.

Graphical Abstract

This is an open access article under the CC BY-NC-ND license (<http://creativecommons.org/licenses/by-nc-nd/4.0/>).

*Correspondence: m-resh@ski.mskcc.org.

AUTHOR CONTRIBUTIONS

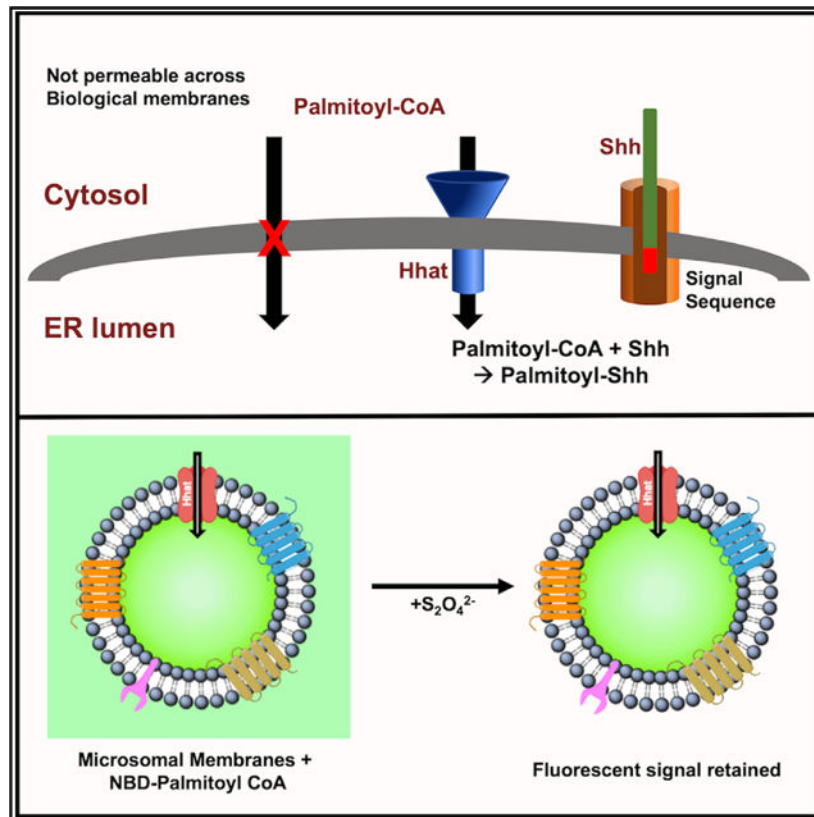
M.D.R. designed the experimental plan. J.J.A. performed the experiments. M.D.R. and J.J.A. analyzed the data and wrote the article.

DECLARATION OF INTERESTS

The authors declare no competing financial interests. TDI-3410 is covered under US Patent application 201662351176: "Hedgehog Acyltransferase inhibitors and uses thereof," filed on 2017-06-16 by Memorial Sloan Kettering Cancer Center and the Tri-Institutional Therapeutics Discovery Institute, Inc.

SUPPLEMENTAL INFORMATION

Supplemental Information can be found online at <https://doi.org/10.1016/j.celrep.2019.11.110>.



In Brief

Palmitoylation of hedgehog proteins by Hedgehog acyltransferase (Hhat) occurs on the luminal side of the ER. However, the palmitoyl-CoA donor for the reaction is membrane impermeable. Asciolla and Resh show that Hhat serves a dual function as both an acyltransferase and a transporter that promotes palmitoyl-CoA uptake across the ER membrane.

INTRODUCTION

The Hedgehog family of secreted signaling proteins plays a fundamental role during embryonic development, acting as morphogens to form concentration gradients for long-range and short-range signaling (McMahon et al., 2003; Fuccillo et al., 2006). Three Hedgehog proteins are expressed in vertebrates—Sonic (Shh), Indian (Ihh), and Desert (Dhh)—with Shh being the most extensively characterized family member. Shh signaling regulates cellular proliferation and differentiation, particularly during limb development and developmental patterning of the brain (Chiang et al., 1996; Roessler et al., 1997). In adults, aberrant Shh expression is associated with multiple human cancers, including medulloblastoma, pancreatic, and lung cancers (Justilien and Fields, 2015; Jiang and Hui, 2008; Mathew et al., 2014).

Formation of the mature Shh ligand involves multiple processing steps, beginning with the removal of the N-terminal signal peptide during translocation across the endoplasmic reticulum (ER) membrane (Mann and Beachy, 2004). Upon entry into the ER, the 45-kDa

Shh precursor undergoes autocleavage to produce a 19-kDa product. Concomitant with autocleavage, cholesterol is attached to the C terminus of Shh (Porter et al., 1996). In a separate step, the N-terminal cysteine of Shh is modified by the attachment of the 16-carbon fatty acid palmitate, a reaction catalyzed by Hedgehog acyltransferase (Hhat) (Chamoun et al., 2001; Pepinsky et al., 1998; Buglino and Resh, 2008). Palmitoylation of Shh by Hhat is essential for short- and long-range Shh signaling in development and tumorigenesis (Dawber et al., 2005; Lee et al., 2001; Chen et al., 2004; Goetz et al., 2006).

Hhat is an ER-resident multipass membrane protein consisting of 10 transmembrane domains and 2 re-entrant loops (Matevossian and Resh, 2015a). It is a member of the membrane bound-*O*-acyltransferase (MBOAT) family of enzymes that catalyze the attachment of specific fatty acids to secreted proteins (e.g., Porcupine acylation of Wnt proteins; ghrelin *O*-acyltransferase [GOAT] acylation of ghrelin) or intracellular lipids (e.g., acylation of cholesterol by Acyl-CoA cholesterol acyltransferase [ACAT]; acylation of lysophospholipids by DGAT1) (Hofmann, 2000; Buglino and Resh, 2012). Several lines of evidence indicate that MBOAT-catalyzed fatty acylation reactions occur in the lumen of the ER (Csala et al., 2007). A conserved histidine residue essential for acyltransferase activity of all MBOAT proteins is located on the luminal face of the ER membrane, implying that the ER lumen is the location of the enzymes' active site (Shindou et al., 2009). Entry of Shh into the ER is essential for Shh palmitoylation, as Shh lacking an N-terminal signal sequence is not palmitoylated (Buglino and Resh, 2008). It is not known how palmitoyl-coenzyme A (CoA), the palmitate donor for Hhat, enters the ER lumen. Palmitate is esterified to palmitoyl-CoA in the cytosol, but long-chain acyl CoA esters are not permeable across biological membranes (Bavdek et al., 2015; Polokoff and Bell, 1978). Analysis of Hhat transmembrane domain topology revealed the presence of 10 transmembrane domains, 2 re-entrant loops, and multiple loops facing the cytoplasm that constituted a large fraction of the total Hhat protein sequence (Konitsiotis et al., 2015; Matevossian and Resh, 2015). We speculated that this topological complexity might serve to provide a second function for Hhat, namely, to assist in palmitoyl-CoA uptake for delivery to the ER lumen. Here, we use assays with microsomal membranes, purified Hhat reconstituted into liposomes, and live cells to support the hypothesis that Hhat itself promotes palmitoyl-CoA entry across the ER membrane. These findings reveal a key role for Hhat in the essential process of transporting a membrane impermeant long-chain fatty acyl CoA across the ER membrane to the luminal side, where it is subsequently used as a substrate for acylation of Shh and potentially of other MBOAT substrates.

RESULTS

Hhat Promotes Palmitoyl-CoA Uptake in Microsomal Membranes

To test the hypothesis that Hhat promotes palmitoyl-CoA uptake across the ER membrane, we devised an assay to track fatty acyl CoA transfer into intact microsomes (Figure 1A). Cellular homogenization results in fragmentation of the ER; the ER fragments then reseal right-side out to form closed membrane vesicles known as microsomes (DePierre and Ernster 1977). Microsomal membranes were prepared from HEK293FT cells transfected with empty vector (EV; pcDNA3.1) or cDNA constructs encoding hemagglutinin (HA)-

with Etomoxir, a selective, small-molecule inhibitor of CPT1 (Figure 2F). The effects of Etomoxir and TDI-3410 on palmitoyl-CoA uptake were additive; treatment with both compounds reduced the NBD signal to baseline levels. A reduction in NBD-palmitoyl-CoA uptake in membranes from EV cells treated with CPT1 inhibitors was not apparent in Figure 2F, but the relative fluorescence units (RFU) values were low and close to baseline, obscuring any potential effect. When the gain on the plate reader was increased in order to more accurately capture low-intensity signals, a reduction in NBD-palmitoyl-CoA uptake in both control (EV) and Hhat membranes by Etomoxir was evident (Figure 2G). Etomoxir had no effect on Shh palmitoylation by purified Hhat (Figure 2H). These data imply that microsomal membranes contain a mixed population of mitochondria and the ER in which the uptake of palmitoyl-CoA is mediated by CPT1/2 and Hhat, respectively. We were not able to efficiently separate mitochondria from Hhat-containing ER membranes with sufficient purity to distinguish between mitochondrial and ER uptake. Therefore, as a next step, we tested the effect of Hhat loss on palmitoyl-CoA uptake.

Microsomal Membranes from Hhat^{-/-} Cells Exhibit Reduced Palmitoyl-CoA Uptake

To evaluate the role of endogenous Hhat in the uptake of palmitoyl-CoA into the ER, NBD-palmitoyl-CoA and ¹²⁵I-Iodopalmitoyl-CoA uptake assays were performed with microsomal membranes generated from T47D breast cancer cells in which Hhat was knocked out using CRISPR/Cas9. Palmitoyl-CoA uptake was decreased by 40%–55% in membranes generated from Hhat^{-/-} T47D cells, compared to membranes from control (Hhat-expressing) cells (Figures 3A and 3B). Treatment with 10 μM TDI-3410 had no effect on the amount of NBD-palmitoyl-CoA uptake into Hhat^{-/-} membranes, compared to DMSO, consistent with the absence of Hhat, the target for TDI-3410. Treatment of the Hhat^{-/-} membranes with 10 μM Etomoxir reduced the NBD signal, and the addition of TDI-3410 had no further effect. These findings imply that in the absence of Hhat, the observed palmitoyl-CoA uptake signal mostly represents uptake into mitochondria. Similar results were obtained using microsomal membranes generated from murine embryonic fibroblast (MEFs) derived from Hhat knockout mice (Chen et al., 2004; Figures 3C and 3D). No uptake of NBD-palmitoyl-CoA was detected when membranes from either WT or Hhat^{-/-} MEFs were incubated at 0°C (Figure 3E), consistent with a transport-like function of Hhat in promoting the uptake of palmitoyl-CoA across the ER membrane.

Purified Hhat Reconstituted into Liposomes Mediates Palmitoyl-CoA Uptake

To definitively test the ability of Hhat to promote palmitoyl-CoA uptake, we purified Hhat (Buglino and Resh, 2008) and reconstituted the purified protein into 200-nm-large unilamellar liposomes containing a membrane lipid composition reflective of the ER (Davison and Wills, 1974; van Meer et al., 2008). We calculated that approximately 12 molecules of Hhat were incorporated per 200-nm liposome. As a control, a parallel, mock purification was performed using cells transfected with the EV. The uptake of NBD-palmitoyl-CoA and ¹²⁵I-Iodopalmitoyl-CoA was 5-fold greater in liposomes reconstituted with purified WT Hhat, compared to liposomes reconstituted with the EV preparation or with the purified H379A Hhat mutant (Figures 4A and 4B). A similar result was obtained with [¹⁴C]-palmitoyl-CoA (Figure 4C). The addition of 10 μM TDI-3410 inhibited NBD-palmitoyl-CoA uptake, with an IC₅₀ of 2.45 μM (Figures 4A and 4D). This value is

comparable to the IC₅₀ of TDI-3410 for the inhibition of Shh palmitoylation (Figure 2D). Etomoxir had no detectable effect on palmitoyl-CoA uptake into the Hhat-containing liposomes or on Shh palmitoylation activity of purified Hhat (Figures 2H and 4A).

We performed several controls to ensure that the fluorescent signal detected in liposomes with reconstituted Hhat represented the NBD-palmitoyl-CoA that entered the liposome interior. The integrity of the liposomal bilayer was evaluated by taking RFU readings every 2 min for 2 h after the quencher was added. The readings remained constant, implying that there was little to no leakage of the quencher or NBD-palmitoyl-CoA through the membrane and that the membrane bilayer remained sealed throughout the experiment (Figure 4E). To test the possibility that the fluorescent signal reflected NBD associated with the external leaflet of the liposome membrane that was protected from the quencher, NBD-phosphatidylcholine (PC), a fluorescent phospholipid that cannot permeate the bilayer, was added to the liposomes. No significant signal above baseline was observed for either Hhat-containing or empty liposomes that were incubated with NBD-PC (Figure 4F). We monitored the Hhat orientation within liposomes by purifying and reconstituting 157FLAG Hhat, an Hhat construct with a FLAG epitope tag located in a loop on the luminal side of the membrane (Matevossian and Resh, 2015a). The treatment of intact liposomes with trypsin had no effect on the FLAG signal in the absence of detergent. Upon the addition of octyl glucoside, the FLAG signal was eliminated (Figure 4G). These data suggest that Hhat molecules are uniformly oriented in a manner similar to that of ER microsomes.

Next, we formed empty or Hhat-reconstituted liposomes in the presence of dithionite. External dithionite was removed, resulting in liposomes containing Hhat with the quencher only in the interior (Figure 5A). A 7-fold decrease in the NBD signal was observed after the incubation of Hhat-reconstituted liposomes with NBD-palmitoyl-CoA compared to empty liposomes, consistent with the interpretation that NBD-palmitoyl-CoA had crossed the vesicle membrane, and the signal had then been quenched (Figure 5B). Treatment with 10 μM TDI-3410 prevented the quenching-dependent decrease in fluorescent signal observed without the drug (Figure 5B), and the addition of 0.2% octylglucoside reduced the NBD signal to baseline (Figure 5B). These findings provide direct evidence that Hhat promotes palmitoyl-CoA uptake across a membrane bilayer and support the hypothesis that Hhat can function as a transporter in addition to its enzymatic activity as an acyltransferase.

To determine the effect of Shh substrate on transport activity, Hhat was reconstituted into liposomes containing the quencher and either buffer, WT, or C24A Shh peptide inside (representing the luminal location of Shh in cells). The external quencher and peptide were removed, NBD-palmitoyl-CoA was added to the outside of the liposomes, and the fluorescent signal was monitored for 2 h. A time-dependent reduction in the NBD signal was evident in liposomes reconstituted with Hhat, whereas little change occurred in the control (EV) liposomes (Figure 5C). Hhat liposomes containing WT Shh peptide, a substrate for Hhat, accumulated less NBD-palmitoyl-CoA than did liposomes that did not contain the Shh peptide. In the presence of C24A Shh peptide, which lacks the Cys palmitoylation site and cannot be palmitoylated by Hhat, minimal uptake of NBD-palmitoyl-CoA occurred. A similar result was obtained by monitoring the uptake of [¹⁴C]-palmitoyl-CoA into liposomes reconstituted with purified Hhat. The uptake of [¹⁴C]-palmitoyl-CoA was 4-fold greater in

liposomes reconstituted with purified WT Hhat, compared to liposomes reconstituted with the EV preparation or with the purified H379A Hhat mutant (Figure 4C). The presence of the WT Shh peptide inside the liposome reduced the amount of palmitoyl-CoA accumulation, whereas the C24A mutant Shh peptide prevented nearly all palmitoyl-CoA uptake (Figure 5D). These data indicate that palmitoyl-CoA transport activity of Hhat is regulated by the Shh substrate. Transport is reduced when Hhat is engaged in acyltransferase catalysis, likely a result of the binding of Shh to Hhat and the release of the palmitoylated Shh product. The C24A Shh mutant cannot be palmitoylated and remains bound to the enzyme, thereby blocking transport activity.

Visualization of Palmitoyl-CoA Uptake by Liposomes Containing Purified, Reconstituted Hhat

To directly visualize NBD-palmitoyl-CoA associated with a liposome, we generated liposomes with fluorescently labeled phosphatidylethanolamine (Cy5.5-PE) incorporated into the liposomal membrane. The addition of Cy5.5-PE did not affect the NBD signal when readings were taken at an excitation of 460 nm and an emission of 535 nm (Figure 6A). Liposomes consisting of reconstituted Hhat and Cy5.5-PE integrated into the liposomal membrane exhibited Hhat-dependent palmitoyl-CoA uptake that was inhibited by TDI-3410, similar to the uptake observed with non-Cy5.5-PE labeled liposomes (Figure 6B). Confocal microscopy was then used to image single liposomes. In liposomes reconstituted with Hhat, sequential Z stacks revealed NBD fluorescence surrounded by Cy5.5-PE in the liposome membrane (Figure 6C; Video S1). A line scan for a central Z stack revealed that the green (NBD) signal lies within the limits of the red (Cy5.5) signal (Figure 6D). Since the size of the liposomes is close to the resolution limit of light microscopy, these results could reflect NBD-palmitoyl-CoA bound to Hhat and/or the inner bilayer leaflet or NBD-palmitoyl-CoA that was transported through the membrane. Because of the limit in resolution, it is not possible to distinguish fluorescence from NBD-palmitoyl-CoA bound to the inner leaflet versus that within the liposome interior. No detectable NBD signal was observed in the control, empty liposomes (Figure 6C). Taken together, these experiments provide strong evidence for a role for Hhat in promoting the uptake of palmitoyl-CoA across a phospholipid bilayer.

Visualization of Palmitoyl-CoA Uptake into the ER of Cells Expressing Hhat

We next asked if Hhat-mediated palmitoyl-CoA uptake into the ER could be visualized within live cells. Cells were first treated with low concentrations of digitonin, a detergent that selectively permeabilizes the plasma membrane while leaving internal membranes intact (Matevossian and Resh, 2015a; Ronning et al., 1982). Next, NBD-palmitoyl-CoA was added along with ER-Tracker Red (glibenclamide BODIPY TR), and after a 60-min incubation, the cells were washed. Live confocal imaging revealed an extensive colocalization of NBD fluorescence with the ER marker in cells overexpressing Hhat, which was dissipated upon the addition of octyl glucoside (Figure 7A). Little to no detectable NBD fluorescence was observed in cells transfected with the EV or H379A Hhat or in cells treated with TDI-3410.

Separation of Hhat Channel Activity from Enzymatic Activity

A recent report described the 3-dimensional crystal structure of DltB, a bacterial MBOAT enzyme that catalyzes the attachment of D-Ala to the cell wall peptidoglycan of Gram-positive bacteria (Ma et al., 2018). The structure is notable for the presence of a funnel and tunnel that extend through the bilayer and potentially connect the intracellular and extracellular sides of the membrane. DltB, like Hhat, needs to perform cross-membrane catalysis, as D-Ala is produced on the opposite side of the membrane from the peptidoglycan substrate to which it is attached. Several of the funnel/tunnel residues in DltB are conserved in mammalian MBOAT proteins, including H379 and Y351 in Hhat. H336, the DltB equivalent of H379, sits at the bottom of the extracellular funnel, whereas F301 (Y351 in Hhat) is localized within the DltB tunnel. Both Hhat mutants were defective in Hhat-mediated palmitoyl-CoA uptake into microsomal membranes (Figures 7B and S2). The effect of these mutations was then tested on Hhat-mediated Shh palmitoylation. We first monitored the ability of the Hhat mutants to palmitoylate Shh in intact cells, where ^{125}I -Iodopalmitate must be converted to ^{125}I -Iodopalmitoyl CoA and then cross the ER membrane to gain access to the lumen. Incorporation of ^{125}I -Iodopalmitate into Shh was strongly reduced for both Y351A and H379A Hhat mutants (Figure 7C), consistent with the need for Hhat to perform both palmitoyl-CoA uptake and acyltransferase activity on the luminal side of the ER in an intact cell, as well as intact microsomes. To determine if Hhat channel activity could be separated from acyltransferase activity, we used Hhat-containing microsomal membranes to compare Shh palmitoylation activities of the mutants to WT Hhat. This *in vitro* assay uses an N-terminal Shh peptide and ^{125}I -Iodopalmitoyl-CoA. It is performed with a buffer that contains detergent to permeabilize the membrane and allow the Shh peptide to access the catalytic site of Hhat. As reported previously (Buglino and Resh, 2008), H379A Hhat exhibited compromised Shh palmitoylation activity, consistent with the notion that H379 is an active site residue. By contrast, Y351A retained near-WT levels of Shh palmitoylation activity when assayed *in vitro* using detergent-solubilized membranes and as a purified enzyme (Figures 7D and 7E). These observations indicate that the uptake of palmitoyl-CoA and acyltransferase activity can be separated and represent dual functions of Hhat.

DISCUSSION

Hhat was originally identified as a palmitoyl acyltransferase for Hedgehog proteins. In this study, we provide multiple lines of evidence to support the hypothesis that Hhat also functions to promote palmitoyl-CoA access to the luminal side of the ER membrane. Fluorescent-based and radioactivity-based assays encompassing three complementary fatty acyl CoA probes—NBD-palmitoyl-CoA, ^{125}I -Iodopalmitoyl-CoA, and [^{14}C]-palmitoyl-CoA—demonstrated that Hhat overexpression increased palmitoyl-CoA uptake into microsomal vesicles. Palmitoyl-CoA uptake was inhibited by treatment with the small-molecule Hhat inhibitor TDI-3410 and was compromised in microsomal membranes prepared from cells overexpressing H379A Hhat, a catalytically inactive Hhat mutant. Moreover, the uptake of palmitoyl-CoA was reduced in microsomal vesicles generated from cells in which Hhat had been depleted. Reconstitution of purified Hhat into artificial phospholipid vesicles provided evidence that palmitoyl-CoA uptake activity was directly due

to the presence of Hhat, and confocal imaging of the liposomes as well live imaging of semi-intact cells confirmed these findings. We conclude that Hhat promotes the uptake of palmitoyl-CoA to the luminal side of the ER membrane, where it is used as a substrate for Hhat-mediated palmitoylation of the Shh protein.

Palmitoyl-CoA Is Not Intrinsically Permeable across Biological Membranes

Palmitoylation of Shh by Hhat has been shown to occur within the ER (Buglino and Resh, 2008). Thus, both substrates for Hhat, palmitoyl-CoA and Shh, must gain access to the ER lumen. Shh enters the lumen of the ER via engagement of its signal peptide with the secretory machinery, but long-chain fatty acids such as palmitoyl-CoA are not permeable across biological membranes (Bavdek et al., 2015; Polokoff and Bell, 1978). To date, the mechanism by which palmitoyl-CoA accesses the lumen of the ER so that Shh palmitoylation can occur remains unknown.

In mitochondria, the CPT system is responsible for the transfer of palmitoyl-CoA across the inner and outer mitochondrial membranes into the matrix. CPT1 first catalyzes the transfer of palmitate from coenzyme A to carnitine-forming palmitoylcarnitine, which subsequently diffuses across the outer mitochondrial membrane (Bremer, 1963). Carnitine-acylcarnitine translocase then shuttles the palmitoylcarnitine across the inner mitochondrial membrane, where it is converted back into palmitoyl-CoA by the enzyme CPT2 (Murthy and Pande, 1990). CPT1 has been reported to be exclusively localized to mitochondria, with the exception of the CPT1c isoform, which was detected in the ER membrane in mouse neuronal cells (Sierra et al., 2008; Broadway et al., 2003). We tested whether a similar system was operative in Hhat-containing microsomal membranes. Treatment with Etomoxir or malonyl-CoA partially inhibited palmitoyl-CoA uptake, indicating that a portion of the NBD signal protected by the quencher represented a CPT1-dependent uptake of palmitoyl-CoA. The remainder of the signal was reduced to baseline by the further addition of TDI-3410. Etomoxir, but not TDI-3410, inhibited NBD-palmitoyl-CoA uptake in Hhat-depleted cells (Figure 3). These findings suggest that at least two mechanisms for palmitoyl-CoA uptake are operative in microsomes: CPT1-mediated uptake into mitochondria and Hhat-mediated uptake into the ER. We were able to separate mitochondria from the ER based on differential centrifugation and organelle markers (HSP60 for mitochondria; protein disulfide isomerase for the ER). However, a considerable amount of Hhat was present in the “heavy” membrane fraction, which may reflect Hhat multimers in dense regions of the ER and/or Hhat localized to ER-mitochondrial contact points. The use of purified Hhat reconstituted into liposomes clearly established that Hhat can promote palmitoyl-CoA uptake into a closed-membrane vesicle in the absence of CPT1.

Given the complex transmembrane topology of MBOAT proteins, it is possible that the overexpression of a multipass transmembrane protein such as Hhat might artificially induce membrane permeability or leakage. However, overexpression of the Wnt acyltransferase Porcupine, another multipass MBOAT protein, had no effect on NBD-palmitoyl-CoA uptake into microsomes. Moreover, time course experiments demonstrated that the integrity of the membranes was not compromised after 120 min (Figure S1A). Finally, imaging of Hhat-containing liposomes with confocal microscopy is consistent with the presence of an intact

bilayer, as fluorescence would have been immediately quenched in the event of liposomal leakage.

Hhat Possesses Both Shh Palmitoylation and Palmitoyl-CoA Uptake Activity

Palmitoyl-CoA uptake was inhibited by both TDI-3410, a small-molecule Hhat inhibitor, and in membranes containing Hhat H379A, a catalytically defective Hhat mutant. This suggests that the two activities, palmitoyl acyltransferase and palmitoyl-CoA uptake, might be linked. We explored this possibility using two mutants of Hhat. Hhat H379A has been shown to be catalytically compromised when assayed for Shh palmitoylation activity *in vitro* and in cells (Buglino and Resh, 2008, 2010). Here, we show that palmitoyl-CoA uptake into microsomal membranes as well as Hhat-containing liposomes expressing this mutant was similarly compromised, suggesting that H379 is critical for both catalytic activity and transport activity. However, Hhat Y351A displayed <25% of WT activity for both Shh palmitoylation and NBD-palmitoyl-CoA uptake in cells but exhibited near-WT Shh palmitoylation activity *in vitro*. The difference can be explained by the difference in membrane integrity in the two assays. In cell-based assays, the ER membrane is intact, and Shh palmitoylation is dependent upon palmitoyl-CoA delivery across the ER membrane. Disruption of membrane integrity by detergent in the *in vitro* palmitoylation assay buffer allows the access of Hhat substrates to the interior of membrane vesicles. Under these conditions, Y351A Hhat is fully active as a Shh palmitoyl transferase. This was not the result of Y351A Hhat stabilizing or activating any endogenous Hhat in the membrane, as the acyltransferase activity of purified Y351A Hhat was equivalent to that of purified WT Hhat (Figure 7E).

Regulation of Hhat-Mediated Palmitoyl-CoA Transport

Based on the laws of thermodynamics, one would expect transport to be bidirectional (i.e., palmitoyl-CoA should constantly exchange in and out of the vesicle). However, after steady state was reached, there was no reduction in the NBD signal in the presence of an external quencher, implying that transport is unidirectional and that palmitoyl-CoA accumulates inside the vesicle. This supposition is consistent with the hydrophobic nature of palmitoyl-CoA and its ability to bind tightly to and be retained on membranes. While the thermodynamics of transport of soluble compounds allows for bidirectionality, hydrophobic compounds behave differently. Palmitoyl-CoA that enters the lumen through Hhat would be captured and retained by hydrophobic binding to the inner leaflet of the membrane bilayer. Strong hydrophobic binding to the lipid bilayer reduces the kinetic “off rate,” resulting in trapping at the membrane. This mechanism, known as kinetic bilayer trapping, is exhibited by lipidated proteins and peptides. For example, the off rate for a palmitoylated peptide bound to a lipid bilayer is extremely slow, with an estimated half-time of 155 h (Schroeder et al., 1997). In our experiments, the NBD signal in microsomes (Figure S1A) and liposomes (Figure 4E) containing Hhat remained constant for up to 2 h after the quencher was added. If transport was bi-directional, NBD-palmitoyl-CoA fluorescence would be quenched as it exited the liposomes (or microsomes), and the signal would decrease over time.

Calculating the stoichiometry of palmitoyl-CoA uptake allows us to distinguish between the binding of fatty acyl CoA to Hhat and the transport through the membrane. The turnover for

Hhat-mediated transport—calculated based on the amount of palmitoyl-CoA retained in the liposome, the number of liposomes in the assay, and the number of Hhat molecules per liposome—is 18–23 molecules of palmitoyl-CoA transported per molecule of Hhat. These numbers support the contention that transport is non-stoichiometric, with multiple turnovers of Hhat allowing palmitoyl-CoA to accumulate on the luminal side of the vesicle membrane. The starting concentration of palmitoyl-CoA on the outside of the liposome was 8 μM , and net uptake by Hhat resulted in a concentration within liposomes of $\sim 100 \mu\text{M}$. Liposome integrity remained intact over 2 h, consistent with findings that large unilamellar vesicles cannot be lysed even at palmitoyl-CoA:lipid ratios of 1.6:1 (Bavdek et al., 2015); the ratio in our experiments is 0.01:1. Total concentrations of long-chain fatty acyl CoAs in the cytoplasm are estimated to be 5–160 μM , but the effective free concentration in the cytosol is $\sim 200 \text{ nM}$, due to binding to membranes and fatty acyl CoA-binding proteins (Knudsen et al., 1999). Within the lumen of the ER, it is likely that palmitoyl-CoA is bound to the inner bilayer leaflet but may also associate with binding partners yet to be identified.

Palmitoyl-CoA uptake monitored in the absence of Shh substrate likely represents transport by Hhat in an “open” conformation. When the Shh substrate binds to the enzyme on the luminal side, Hhat engages in acyltransferase activity, and some of the palmitoyl-CoA delivered through the tunnel is diverted to acylate Shh. This is consistent with the predicted location of the catalytic His379 residue at the base of the funnel and may reflect the transfer of palmitate to Shh within the tunnel/funnel (Ma et al., 2018). The fate of the CoA moiety released after the palmitate transfer to Shh is not known. A probe that specifically detects free CoA inside the vesicle would be required to determine if CoA is released into the lumen or to the cytosolic side of the membrane. Dissociation of the palmitoylated Shh product from the enzyme allows for another round of transport and catalysis. By contrast, mutant Shh binds to Hhat but cannot be released from the enzyme, thereby blocking the tunnel and preventing the entry of palmitoyl-CoA. Thus, acyltransferase and fatty acyl CoA transport activities are linked and coordinated.

MBOAT Family Enzymes as Tunnels

A recent study provided a three-dimensional crystal structure of DltB, an MBOAT family protein responsible for the D-alanylation of cell wall teichoic acid in Gram-positive bacteria (Ma et al., 2018). The structure reveals a tunnel/funnel within DltB that may provide an opening for substrate transit from one side of the bacterial membrane to the other. A comparison of Hhat and DltB sequences revealed conserved residues that may be located in a tunnel/funnel of Hhat and might be important for transport activity. The DltB equivalent of Hhat H379 is located at the base of the funnel near the membrane interface, which could explain why it is compromised in both catalytic and transport activity. The Hhat Y351 equivalent of DltB is located higher up in the funnel, which might affect transport activity without affecting catalytic activity. The evidence provided in this study suggests that Hhat might adopt a similar tunnel/funnel structure as DltB. Thus, Hhat could operate as a carrier for palmitoyl-CoA from the cytosol, where it is produced, to the ER lumen. This would provide a biochemical mechanism for transmembrane catalysis not only by Hhat, but also for other ER enzymes dependent on a luminal source of palmitoyl-CoA.

Three members of the MBOAT family—Hhat, Porcupine, and GOAT—transfer fatty acids to secreted proteins. The two-dimensional transmembrane topology maps of Hhat and GOAT are remarkably similar, and it is likely that Porcupine has a similar topology (Matevossian and Resh, 2015a; Konitsiotis et al., 2015; Taylor et al., 2013; Rios-Esteves et al., 2014). Based on similarities to DltB, Porcupine and GOAT may also have a tunnel to promote the uptake of their respective fatty acyl CoA substrates from the cytosol across the ER membrane. The tunnel would be expected to be selective with regard to fatty acyl chain length and saturation, since Porcn does not promote palmitoyl-CoA uptake into microsomal vesicles (Figure 2), nor does it use palmitoyl-CoA as a substrate for Wnt acylation (Asciolla et al., 2017). Other MBOAT family members that rely on a luminal source of palmitoyl-CoA include DGAT1 and ACAT2 (Csala et al., 2007). These enzymes are predicted to be less topologically complex than Hhat, based on two-dimensional topology maps (McFie et al., 2010; Joyce et al., 2000; Lin et al., 2003). In addition, the glycosyl phosphatidylinositol anchor intermediate, GlcN-acylPI, is produced by the inositol acyltransferase PIG-W in mammalian cells and Gwt1p in yeast using luminal palmitoyl-CoA (Sagane et al., 2011; Murakami et al., 2003). Of note, Hhat is expressed in many adult cell types that do not express detectable levels of Hedgehog proteins. It is tempting to speculate that Hhat serves as a conduit to provide luminal palmitoyl-CoA not only for other MBOATs such as DGAT and ACAT2, but also for other enzymes that catalyze luminal palmitoyl-CoA reactions.

STAR★METHODS

LEAD CONTACT AND MATERIALS AVAILABILITY

Further information and requests for resources and reagents should be directed to and will be fulfilled by the Lead Contact, Dr. Marilyn D. Resh (m-resh@ski.mskcc.org). There are restrictions to the availability of TDI-3410, due to the lack of an external centralized repository for its distribution, the limited quantities available and our need to maintain the stock. We are glad to share TDI-3410 with reasonable compensation by the requestor for its processing and shipping and a completed Materials Transfer Agreement.

EXPERIMENTAL MODEL AND SUBJECT DETAILS

Cell and cell lines—COS-1 (CRL-1650) and COS-7 (CRL-1651) cells were obtained from the ATCC, and were grown in Dulbecco's Modified Eagle's (DMEM) medium supplemented with 10% fetal bovine serum, 1 mM GlutaMAX (Invitrogen), 50 units/ml penicillin, and 50 g/ml streptomycin. HEK293FT cells, purchased from Invitrogen (R70007), were grown in Dulbecco's modified Eagle's medium supplemented with 10% fetal bovine serum, 50 units/ml penicillin, 50 mg/ml streptomycin, 500 µg/ml Geneticin, 1 mM GlutaMAX (Invitrogen), 1 mM sodium pyruvate, and 0.1 mM nonessential amino acids. T47D cells (ATCC HTB-133) were authenticated using Short Tandem Repeat (STR) analysis by the ATCC Cell Line Authentication Service. T47D cells were grown in RPMI-1640 supplemented with 10% fetal bovine serum, 0.2 Units/ml bovine insulin. HHAT ^{-/-} T47D cells were generated using Origene CRISPR Kit# KN208447. HHAT ^{-/-} MEFs were a kind gift of Dr. Pao-Tien Chuang, UCSF.

METHOD DETAILS

Reagents and Antibodies—Bio-Beads SM-2 Adsorbents (1528920), and Econo-Column® Chromatography Columns, 0.5 × 5 cm (7370507) were purchased from Bio-Rad (Hercules, CA). Corning 96-Well Clear Bottom Black Polystyrene Microplates (07-200-565), ProLong Glass Antifade Mountant (P32980), ER-Tracker Red (BODIPY TR Glibenclamide) (E34250), and Triton X-100 (BP151) were purchased from Fisher Scientific (Hampton, NH). Sephadex® G-75 (GE17-0051-01), sodium hydrosulfite (157953), mouse monoclonal Flag-specific (anti-Flag) M2 (F3165; 1:30 for immunoprecipitation), rabbit polyclonal anti-HA antibodies (H6908; 1:1,000), digitonin (D6628), FlagM2 agarose (A2220), and 3 × Flag peptide (F4799) were purchased from Sigma-Aldrich (St. Louis, MO). Octyl glucoside (494459) was purchased from EMD Millipore (Billerica, MA). [¹²⁵I]NaI (NEZ033A005MC) and [¹⁴C]-palmitoyl coenzyme A were purchased from PerkinElmer Life Sciences (Waltham, MA). {N-[(7-nitro-2-1,3-benzoxadiazol-4-yl)-methyl]amino} palmitoyl Coenzyme A (ammonium salt) (810705P), {N-[(7-nitro-2-1,3-benzoxadiazol-4-yl)-methyl]amino} phosphatidylcholine (810130P), cy5.5-phosphatidylethanolamine (810346C), phosphatidylethanolamine (850757P), phosphatidylcholine (840051P), 1-palmitoyl-2-oleoyl-sn-glycero-3-phospho-L-serine (sodium salt) (840034P), and L-α-phosphatidylinositol (Liver, Bovine) (sodium salt) (840042P), were purchased from Avanti Polar Lipids (Alabaster, AL). μ-Slide Angiogenesis (81506) was purchased from ibidi (Madison, WI). Polybrene® (sc-134220) was purchased from Santa Cruz Biotechnology (Dallas, TX). Nunc® Lab-Tek® II chambered coverglass (155382) was purchased from the MSKCC molecular cytology core.

Plasmids, cell culture, transfection, and membrane preparation—The plasmid encoding HA-tagged Hhat was generated as previously described (Buglino and Resh, 2008). Hhat constructs with C-terminal FLAG, His and HA epitope insertions were generated using site-directed mutagenesis via the QuikChange II XL Site directed mutagenesis kit purchased from Stratagene (La Jolla, CA). All constructs were confirmed by DNA sequencing. Cells were transfected with 6 mg of Hhat cDNA using Lipofectamine (Invitrogen), split 1:2 the following day, and then cultured for 24 h. P100 membranes were prepared from hypotonically lysed cells, following centrifugation at 100,000 × g (P100) as described (Buglino and Resh, 2008).

Preparation of Microsomal membranes—HEK293FT cells transfected with EV or Hhat constructs were subjected to hypotonic lysis and a P100 membrane fraction (microsomes) was prepared as described (Buglino and Resh, 2008).

Purification of Recombinant Hhat-HA-Flag-His protein—Purification of wild-type and mutant Hhat-HA-Flag-His protein from transfected HEK293FT cells was carried out as previously described (Buglino and Resh, 2008).

Preparation of 200 nm Liposomes—Lipids, resuspended in chloroform, were mixed in ratios of 50% PC, 30% PE, 10% PI, 10% PS and dried under nitrogen gas. Liposomes were formed by reconstituting phospholipids (10mg of phospholipids dried from 100 μl chloroform) with either wild-type or mutant Hhat in 20 mM HEPES (pH 7.3, 350 mM NaCl,

1% octylglucoside, 1% glycerol) prior to passing through a Bio-Beads SM-2 Adsorbents detergent removal column (Bio-Rad) ten times. Liposomes were then extruded 30 times through a polycarbonate filter with 0.2 μm pore size and subsequently passed through a Econo-Column® Chromatography Column, 0.5 \times 5 cm (Bio-Rad) containing Sephadex® G-75 (Sigma). Six, 1ml fractions were collected, aliquoted, and stored at -80°C . Analysis of Hhat orientation in liposomes was performed as described (Matevossian and Resh, 2015a).

Liposome quantification—The number of lipids in a 200 nm diameter unilamellar liposome was calculated to be 1.9×10^5 :

$$A = \frac{4\pi(d/2)^2 + (d/2 - l)^2}{A_{\text{PL}}}$$

Where d = outer diameter of liposome; l = 5 nm (thickness of the bilayer); A_{PL} = surface area of a phospholipid, assuming 70\AA^2 for DOPC (Nilsson et al., 2016; Nagle and Tristram-Nagle, 2000). The number of liposomes in the assay was calculated based on a starting concentration of 6.7 mM phospholipid (assuming an average mw of 750). Each assay contained 10 μL , which corresponds to 212×10^9 liposomes. The number of molecules of Hhat per liposome was calculated based on the starting material: 250 ng purified Hhat (mw 57,313) in 10 μL = 2.6×10^{12} molecules Hhat/ 212×10^9 liposomes = 12.3 Hhat molecules per liposome. The internal volume of a 200 nm liposome (assuming 5 nm bilayer width) and the volume of a sphere $4/3\pi r^3 = 3.6 \times 10^{-15}$ ml. The internal concentration of palmitoyl-CoA inside the liposome was calculated based on the net uptake of NBD RFU (6009 RFU/ 77.5×10^{12} RFU/mol = 77.6×10^{-12} mol NBD palmitoyl-CoA/ 212×10^9 liposomes \times 3.6×10^{-18} l/liposome = 102 μM NBD-palmitoyl-CoA inside each liposome) and ^{125}I dpm (9.1×10^{-9} Ci/94 Ci/mol = 97 pmol ^{125}I Iodopalmitoyl-CoA/ 212×10^9 liposomes \times 3.6×10^{-18} l/liposome = 127 μM Palmitoyl-CoA inside each liposome). The turnover for palmitoyl-CoA transport by Hhat was calculated for NBD palmitoyl-CoA ($77.6 \text{ pmol}/212 \times 10^9$ liposomes = 220 molecules NBD palmitoyl-CoA/12 molecules Hhat = 18) and ^{125}I Iodopalmitoyl-CoA ($97 \text{ pmol}/212 \times 10^9$ liposomes = 275 molecules NBD palmitoyl-CoA/12 molecules Hhat = 23).

Synthesis of [^{125}I]iodo-palmitate—Radioiodination of iodo-palmitate with [^{125}I] NaI and the synthesis of [^{125}I] iodo-palmitoylCoA were carried out as previously described (Berthiaume et al., 1995; Peseckis et al., 1993). The final concentration of [^{125}I] iodopalmitoylCoA was determined from the absorbance at 260 nm based on an extinction coefficient of $15.4 \times 10^3 \text{ mM}^{-1} \text{ cm}^{-1}$ at 260 nm.

NBD-Palm-CoA Uptake Assay—10 μL of either 200 nm liposomes, or P100 membranes (1 $\mu\text{g}/\mu\text{L}$ total protein) generated from HEK293FT cells transfected with cDNAs encoding empty vector, wild-type Hhat, Y351A Hhat, or H379A Hhat, were added to 80 μL of MES buffer (pH 6.5) and incubated with 8 μM NBD-Palm-CoA for 60 minutes in the dark, at room temperature in a black 96-well, clear bottom plate. 10 μM sodium dithionite was then added to quench external fluorescence not protected by the vesicle interior. Relative

fluorescent units were determined using a Bio Tek Synergy H1 Hybrid Multi-Mode Microplate Reader.

[¹²⁵I] IodoPalmitoyl-CoA and [¹⁴C] Palmitoyl-CoA Uptake Assays—Microsomal membranes (1μg/μl in 10 ml) generated from HEK293FT cells transfected with cDNAs encoding empty vector, wild-type Hhat or H379A Hhat were added to 80 μl of MES buffer and incubated in the presence of 8 μM [¹²⁵I]Iodopalmitoyl-CoA for 60 minutes at room temperature. Membranes were pelleted (78,000 × g) for 15 min at 4°C, and washed three times with 2% BSA to bind unincorporated radiolabeled [¹²⁵I]Iodopalmitoyl-CoA. CPM were quantified using a Perkin Elmer WALAC 2470–0200 Gamma Counter. Liposomes containing reconstituted Hhat were incubated with 8 μM [¹²⁵I]Iodopalmitoyl-CoA or [¹⁴C] palmitoyl CoA for 60 minutes at room temperature and then processed as above.

Shh Palmitoylation Assays—*In vitro* Shh peptide palmitoylation assays were performed as previously described (Buglino and Resh, 2008) in reaction buffer (167 mM MES (pH 6.5), 1.7 mM DTT, 0.083% Triton X-100) containing [¹²⁵I]-Iodopalmitoyl-CoA, biotinylated Shh peptide, and Hhat containing microsomal membranes or purified Hhat. Cell-based Shh palmitoylation assays were performed using COS-1 cells expressing Shh and either pcDNA, Hhat (WT, H379A, Y351A), Shh, or both Hhat and Shh. Cells were cultured in media containing 2% FBS for 60 minutes at 37°C prior to incubation with 15 μCi [¹²⁵I] IodoPalmitate for 4 hours. Cells were lysed and Shh was immunoprecipitated with anti-Shh antibody (Santa Cruz) overnight at 4°C. Immunoprecipitates and lysates were run on an SDS-PAGE gel that was dried and exposed to a phosphor screen for 4 days. Images were obtained using a phosphorimager (GE Typhoon FLA 7000) and radioactivity incorporated into the Shh bands was quantified using ImageJ image processing software.

Confocal imaging of liposomes—Liposome imaging was performed by pre-coating a μ-Slide Angiogenesis (Ibidi) overnight with polybrene (1:100) in 10 μM MES buffer. An NBD uptake assay was performed with the liposomes, the reaction contents were transferred to wells in a μ-Slide Angiogenesis and allowed to attach to the well surface overnight, protected from light at 4°C. MES buffer was removed the following day and replaced with a sufficient amount of ProLong Glass Antifade Mountant to cover the surface of the well. The liposomes were imaged using a Leica TCS SP8 confocal microscope and the images were processed using LAS X software.

Selective cell permeabilization and indirect immunofluorescence—To selectively permeabilize the plasma membrane, COS-7 cells were plated on Nunc® Lab-Tek® II chambered coverglass wells and incubated with 65 μg/ml digitonin in KHM (20 mM HEPES (pH 7.4), 110 mM potassium acetate, 2mM magnesium acetate) for 10 min on ice. Cells were then incubated with NBD-palmitoyl-CoA (10μM) for 60 minutes and ER tracker (ER-Tracker Red (BODIPY TR Glibenclamide) (1 μM) for 30 minutes at room temperature. Cells were washed and buffer was replaced with 1 mL of phenol red free DMEM. Cells were imaged using a Leica TCS SP8 confocal microscope and the images were processed using LAS X software.

QUANTIFICATION AND STATISTICAL ANALYSIS

All statistical analyses were performed using GraphPad Prism v8. Each experiment was performed with duplicate or triplicate samples as indicated in the figure legends, and was repeated at least two or three times. Error bars represent standard deviation of the mean. An unpaired Student t test was applied, with $p < 0.05$ considered the level of statistical significance.

DATA AND CODE AVAILABILITY

This study did not generate any unique datasets or code.

Supplementary Material

Refer to Web version on PubMed Central for supplementary material.

ACKNOWLEDGMENTS

This work was supported by NIH grant RO1GM116860 to M.D.R. and a Diversity Supplement to J.J.A.; a grant from the Mr. William H. Goodwin and Mrs. Alice Goodwin and the Commonwealth Foundation for Cancer Research and The Center for Experimental Therapeutics at Memorial Sloan Kettering Cancer Center; and a Cancer Center Core Support grant P30 CA008748 from the National Institutes of Health to Memorial Sloan-Kettering Cancer Center. TDI-3410 used in these studies was provided by the Tri-Institutional Therapeutics Discovery Institute. We thank Raisa Louft-Nisenbaum for expert technical assistance, Vitaly P. Boyko for assistance with confocal microscopy and analysis, and Debra Alston for administrative support.

REFERENCES

- Asciolla JJ, Miele MM, Hendrickson RC, and Resh MD (2017). An *in vitro* fatty acylation assay reveals a mechanism for Wnt recognition by the acyltransferase Porcupine. *J. Biol. Chem* 292, 13507–13513. [PubMed: 28655768]
- Bavdek A, Vazquez HM, and Conzelmann A (2015). Enzyme-coupled assays for flip-flop of acyl-Coenzyme A in liposomes. *Biochim. Biophys. Acta* 1848 (11 Pt A), 2960–2966. [PubMed: 26325346]
- Berthiaume L, Peseckis SM, and Resh MD (1995). Synthesis and use of iodo-fatty acid analogs. *Methods Enzymol.* 250, 454–466. [PubMed: 7651171]
- Bremer J (1963). Carnitine in Intermediary Metabolism. The Biosynthesis of Palmitylcarnitine by Cell Subfractions. *J. Biol. Chem* 238, 2774–2779. [PubMed: 14063302]
- Broadway NM, Pease RJ, Birdsley G, Shayeghi M, Turner NA, and Saggerson ED (2003). The liver isoform of carnitine palmitoyltransferase 1 is not targeted to the endoplasmic reticulum. *Biochem. J* 370, 223–231. [PubMed: 12401113]
- Buglino JA, and Resh MD (2008). Hhat is a palmitoylacyltransferase with specificity for N-palmitoylation of Sonic Hedgehog. *J. Biol. Chem* 283, 22076–22088. [PubMed: 18534984]
- Buglino JA, and Resh MD (2010). Identification of conserved regions and residues within Hedgehog acyltransferase critical for palmitoylation of Sonic Hedgehog. *PLoS ONE* 5, e11195. [PubMed: 20585641]
- Buglino JA, and Resh MD (2012). Palmitoylation of Hedgehog proteins. *Vitam. Horm* 88, 229–252. [PubMed: 22391306]
- Chamoun Z, Mann RK, Nellen D, von Kessler DP, Bellotto M, Beachy PA, and Basler K (2001). Skinny hedgehog, an acyltransferase required for palmitoylation and activity of the hedgehog signal. *Science* 293, 2080–2084. [PubMed: 11486055]
- Chen MH, Li YJ, Kawakami T, Xu SM, and Chuang PT (2004). Palmitoylation is required for the production of a soluble multimeric Hedgehog protein complex and long-range signaling in vertebrates. *Genes Dev.* 18, 641–659. [PubMed: 15075292]

- Chiang C, Litingtung Y, Lee E, Young KE, Corden JL, Westphal H, and Beachy PA (1996). Cyclopia and defective axial patterning in mice lacking Sonic hedgehog gene function. *Nature* 383, 407–413. [PubMed: 8837770]
- Csala M, Marcolongo P, Lizák B, Senesi S, Margittai E, Fulceri R, Magyar JE, Benedetti A, and Bánhegyi G (2007). Transport and transporters in the endoplasmic reticulum. *Biochim. Biophys. Acta* 1768, 1325–1341. [PubMed: 17466261]
- Davison SC, and Wills ED (1974). Studies on the lipid composition of the rat liver endoplasmic reticulum after induction with phenobarbitone and 20-methylcholanthrene. *Biochem. J* 140, 461–468. [PubMed: 4447625]
- Dawber RJ, Hebbes S, Herpers B, Docquier F, and van den Heuvel M (2005). Differential range and activity of various forms of the Hedgehog protein. *BMC Dev. Biol* 5, 21. [PubMed: 16197551]
- DePierre JW, and Ernster L (1977). Enzyme topology of intracellular membranes. *Annu. Rev. Biochem* 46, 201–262. [PubMed: 197876]
- Esser V, Kuwajima M, Britton CH, Krishnan K, Foster DW, and McGarry JD (1993). Inhibitors of mitochondrial carnitine palmitoyltransferase I limit the action of proteases on the enzyme. Isolation and partial amino acid analysis of a truncated form of the rat liver isozyme. *J. Biol. Chem* 268, 5810–5816. [PubMed: 8449947]
- Fuccillo M, Joyner AL, and Fishell G (2006). Morphogen to mitogen: the multiple roles of hedgehog signalling in vertebrate neural development. *Nat. Rev. Neurosci* 7, 772–783. [PubMed: 16988653]
- Goetz JA, Singh S, Suber LM, Kull FJ, and Robbins DJ (2006). A highly conserved amino-terminal region of sonic hedgehog is required for the formation of its freely diffusible multimeric form. *J. Biol. Chem* 281, 4087–4093. [PubMed: 16339763]
- Hofmann K (2000). A superfamily of membrane-bound O-acyltransferases with implications for wnt signaling. *Trends Biochem. Sci* 25, 111–112. [PubMed: 10694878]
- Jiang J, and Hui CC (2008). Hedgehog signaling in development and cancer. *Dev. Cell* 15, 801–812. [PubMed: 19081070]
- Joyce CW, Shelness GS, Davis MA, Lee RG, Skinner K, Anderson RA, and Rudel LL (2000). ACAT1 and ACAT2 membrane topology segregates a serine residue essential for activity to opposite sides of the endoplasmic reticulum membrane. *Mol. Biol. Cell* 11, 3675–3687. [PubMed: 11071899]
- Justilien V, and Fields AP (2015). Molecular pathways: novel approaches for improved therapeutic targeting of Hedgehog signaling in cancer stem cells. *Clin. Cancer Res* 21, 505–513. [PubMed: 25646180]
- Knudsen J, Jensen MV, Hansen JK, Faergeman NJ, Neergaard TB, and Gaigg B (1999). Role of acylCoA binding protein in acylCoA transport, metabolism and cell signaling. *Mol. Cell. Biochem* 192, 95–103. [PubMed: 10331663]
- Konitsiotis AD, Jovanovi B, Ciepla P, Spitaler M, Lanyon-Hogg T, Tate EW, and Magee AI (2015). Topological analysis of Hedgehog acyltransferase, a multipalmitoylated transmembrane protein. *J. Biol. Chem* 290, 3293–3307. [PubMed: 25505265]
- Lee JD, Kraus P, Gaiano N, Nery S, Kohtz J, Fishell G, Loomis CA, and Treisman JE (2001). An acylatable residue of Hedgehog is differentially required in Drosophila and mouse limb development. *Dev. Biol* 233, 122–136. [PubMed: 11319862]
- Lin S, Lu X, Chang CC, and Chang TY (2003). Human acyl-coenzyme A:cholesterol acyltransferase expressed in chinese hamster ovary cells: membrane topology and active site location. *Mol. Biol. Cell* 14, 2447–2460. [PubMed: 12808042]
- Ma D, Wang Z, Merrikh CN, Lang KS, Lu P, Li X, Merrikh H, Rao Z, and Xu W (2018). Crystal structure of a membrane-bound O-acyltransferase. *Nature* 562, 286–290. [PubMed: 30283133]
- Mann RK, and Beachy PA (2004). Novel lipid modifications of secreted protein signals. *Annu. Rev. Biochem* 73, 891–923. [PubMed: 15189162]
- Matevossian A, and Resh MD (2015a). Membrane topology of hedgehog acyltransferase. *J. Biol. Chem* 290, 2235–2243. [PubMed: 25488661]
- Mathew E, Zhang Y, Holtz AM, Kane KT, Song JY, Allen BL, and Pasca di Magliano M (2014). Dosage-dependent regulation of pancreatic cancer growth and angiogenesis by hedgehog signaling. *Cell Rep.* 9, 484–494. [PubMed: 25310976]

- McFie PJ, and Stone SJ (2011). A fluorescent assay to quantitatively measure in vitro acyl CoA:diacylglycerol acyltransferase activity. *J. Lipid Res* 52, 1760–1764. [PubMed: 21653930]
- McFie PJ, Stone SL, Banman SL, and Stone SJ (2010). Topological orientation of acyl-CoA:diacylglycerol acyltransferase-1 (DGAT1) and identification of a putative active site histidine and the role of the n terminus in dimer/tetramer formation. *J. Biol. Chem* 285, 37377–37387. [PubMed: 20876538]
- McGarry JD, and Brown NF (1997). The mitochondrial carnitine palmitoyl-transferase system. From concept to molecular analysis. *Eur. J. Biochem* 244, 1–14. [PubMed: 9063439]
- McMahon AP, Ingham PW, and Tabin CJ (2003). Developmental roles and clinical significance of hedgehog signaling. *Curr. Top. Dev. Biol* 53, 1–114. [PubMed: 12509125]
- Murakami Y, Siripanyapinyo U, Hong Y, Kang JY, Ishihara S, Nakakuma H, Maeda Y, and Kinoshita T (2003). PIG-W is critical for inositol acylation but not for flipping of glycosylphosphatidylinositol-anchor. *Mol. Biol. Cell* 14, 4285–4295. [PubMed: 14517336]
- Murthy MSR, and Pande SV (1990). Characterization of a solubilized malonyl-CoA-sensitive carnitine palmitoyltransferase from the mitochondrial outer membrane as a protein distinct from the malonyl-CoA-insensitive carnitine palmitoyltransferase of the inner membrane. *Biochem. J* 268, 599–604. [PubMed: 2363698]
- Nagle JF, and Tristram-Nagle S (2000). Structure of lipid bilayers. *Biochim. Biophys. Acta* 1469, 159–195. [PubMed: 11063882]
- Nilsson T, Lundin CR, Nordlund G, Adelroth P, von Ballmoos C, and Brzezinski P (2016). Lipid-mediated Protein-protein interactions modulate respiration-driven ATP synthesis. *Sci. Rep* 6, 24113. [PubMed: 27063297]
- Pepinsky RB, Zeng C, Wen D, Rayhorn P, Baker DP, Williams KP, Bixler SA, Ambrose CM, Garber EA, Miatkowski K, et al. (1998). Identification of a palmitic acid-modified form of human Sonic hedgehog. *J. Biol. Chem* 273, 14037–14045. [PubMed: 9593755]
- Peseckis SM, Deichaite I, and Resh MD (1993). Iodinated fatty acids as probes for myristate processing and function. Incorporation into pp60v-src. *J. Biol. Chem* 268, 5107–5114. [PubMed: 8444887]
- Petrova E, Rios-Esteves J, Ouerfelli O, Glickman JF, and Resh MD (2013). Inhibitors of Hedgehog acyltransferase block Sonic Hedgehog signaling. *Nat. Chem. Biol* 9, 247–249. [PubMed: 23416332]
- Polokoff MA, and Bell RM (1978). Limited palmitoyl-CoA penetration into microsomal vesicles as evidenced by a highly latent ethanol acyltransferase activity. *J. Biol. Chem* 253, 7173–7178. [PubMed: 701242]
- Porter JA, Young KE, and Beachy PA (1996). Cholesterol modification of hedgehog signaling proteins in animal development. *Science* 274, 255–259. [PubMed: 8824192]
- Rios-Esteves J, Haugen B, and Resh MD (2014). Identification of key residues and regions important for porcupine-mediated Wnt acylation. *J. Biol. Chem* 289, 17009–17019. [PubMed: 24798332]
- Roessler E, Belloni E, Gaudenz K, Vargas F, Scherer SW, Tsui LC, and Muenke M (1997). Mutations in the C-terminal domain of Sonic Hedgehog cause holoprosencephaly. *Hum. Mol. Genet* 6, 1847–1853. [PubMed: 9302262]
- Rojas Á, Del Campo JA, Clement S, Lemasson M, García-Valdecasas M, Gil-Gómez A, Ranchal I, Bartosch B, Bautista JD, Rosenberg AR, et al. (2016). Effect of Quercetin on Hepatitis C Virus Life Cycle: From Viral to Host Targets. *Sci. Rep* 6, 31777. [PubMed: 27546480]
- Ronning SA, Heatley GA, and Martin TF (1982). Thyrotropin-releasing hormone mobilizes Ca²⁺ from endoplasmic reticulum and mitochondria of GH3 pituitary cells: characterization of cellular Ca²⁺ pools by a method based on digitonin permeabilization. *Proc. Natl. Acad. Sci. USA* 79, 6294–6298. [PubMed: 6815650]
- Sagane K, Umemura M, Ogawa-Mitsuhashi K, Tsukahara K, Yoko-o T, and Jigami Y (2011). Analysis of membrane topology and identification of essential residues for the yeast endoplasmic reticulum inositol acyltransferase Gwt1p. *J. Biol. Chem* 286, 14649–14658. [PubMed: 21367863]
- Schroeder H, Leventis R, Rex S, Schelhaas M, Nägele E, Waldmann H, and Silvius JR (1997). S-Acylation and plasma membrane targeting of the farnesylated carboxyl-terminal peptide of N-ras in mammalian fibroblasts. *Biochemistry* 36, 13102–13109. [PubMed: 9335573]

- Shindou H, Hishikawa D, Harayama T, Yuki K, and Shimizu T (2009). Recent progress on acyl CoA: lysophospholipid acyltransferase research. *J. Lipid Res* 50, S46–S51. [PubMed: 18931347]
- Sierra AY, Gratacós E, Carrasco P, Clotet J, Ureña J, Serra D, Asins G, Hegardt FG, and Casals N (2008). CPT1c is localized in endoplasmic reticulum of neurons and has carnitine palmitoyltransferase activity. *J. Biol. Chem* 283, 6878–6885. [PubMed: 18192268]
- Taylor MS, Ruch TR, Hsiao P-Y, Hwang Y, Zhang P, Dai L, Huang CRL, Berndsen CE, Kim M-S, Pandey A, et al. (2013). Architectural organization of the metabolic regulatory enzyme ghrelin O-acyltransferase. *J. Biol. Chem* 288, 32211–32228. [PubMed: 24045953]
- van Meer G, Voelker DR, and Feigenson GW (2008). Membrane lipids: where they are and how they behave. *Nat. Rev. Mol. Cell Biol* 9, 112–124. [PubMed: 18216768]

Highlights

- Hedgehog acyltransferase (Hhat) promotes the uptake of palmitoyl-CoA across membranes
- Palmitoyl-CoA uptake can occur in the absence of a hedgehog protein substrate
- Palmitoyl-CoA uptake is regulated by and separable from hedgehog palmitoylation
- Hhat serves as a conduit to supply palmitoyl-CoA to the luminal side of the ER

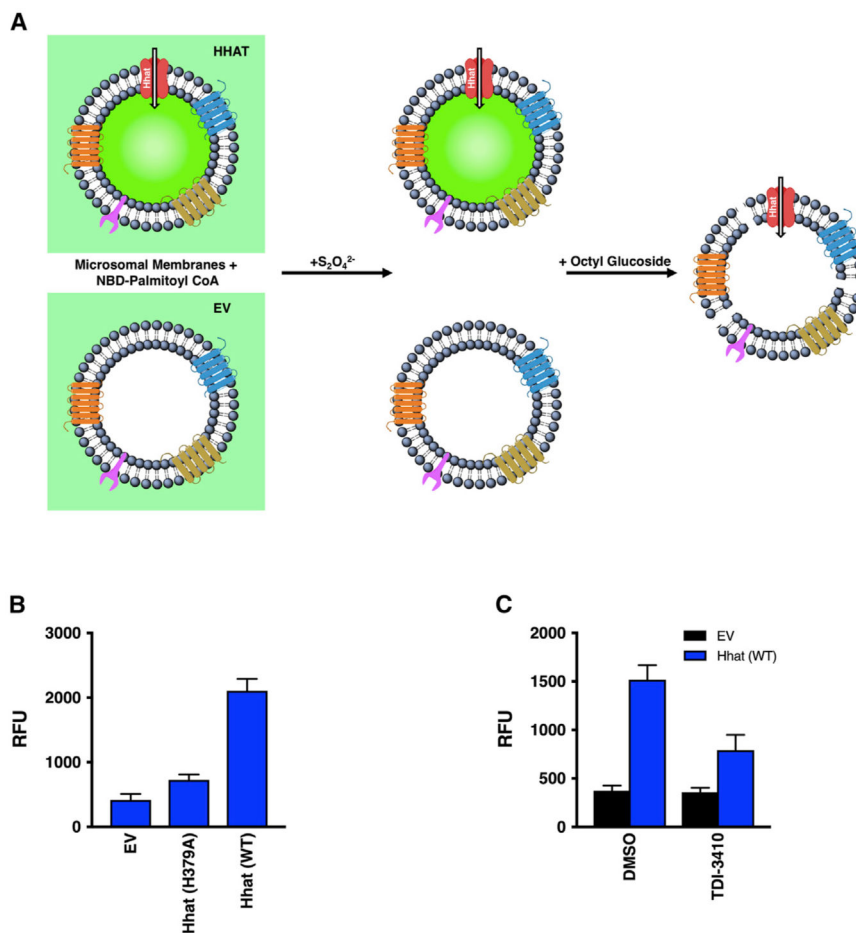


Figure 1. NBD-Palmitoyl-CoA Uptake Assay

(A) Microsomal membranes generated from HEK293FT cells transfected with pcDNA3.1 (empty vector; EV) or pcDNA3.1 encoding Hhat are incubated with NBD-palmitoyl-CoA, then treated with dithionite ($Na_2S_2O_4^{2-}$), a membrane-impermeant reducing agent that quenches NBD fluorescence of molecules on the external side of the membrane. RFU readings at 535 nm reflect NBD-palmitoyl-CoA within the vesicle and protected from the quencher. The addition of 0.2% octyl glucoside permeabilizes the bilayer and allows access of the quencher to the interior of the vesicle.

(B) Microsomal membranes from HEK293FT cells expressing pcDNA, Hhat WT, or Hhat H379A were incubated with NBD-palmitoyl-CoA for 60 min at room temperature prior to the addition of $Na_2S_2O_4^{2-}$. NBD fluorescence in the interior of the vesicles was quantified; $n = 3$.

(C) Microsomal membranes were pretreated for 15 min with 10 μ M TDI-3410, then analyzed for NBD-palmitoyl-CoA; $n = 3$.

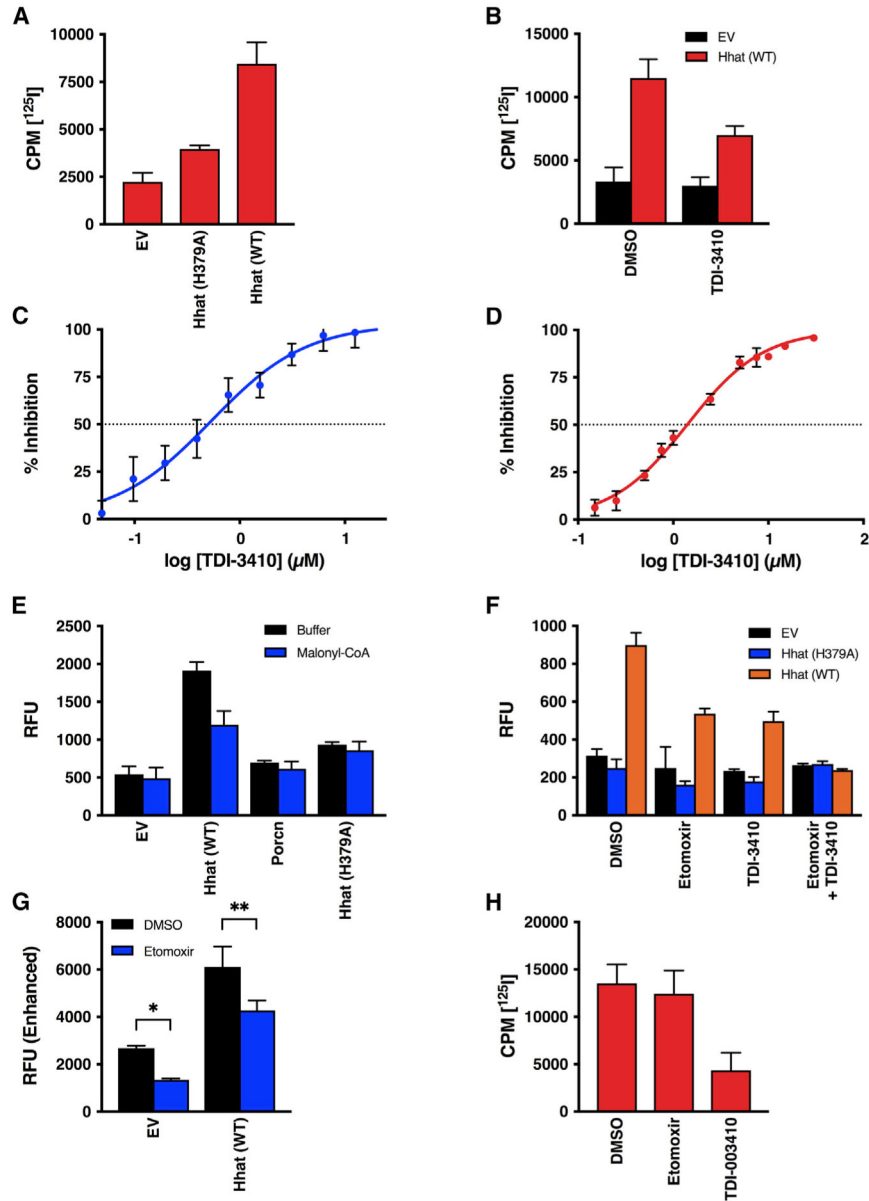


Figure 2. Hhat Enhances Uptake of Palmitoyl-CoA across the ER Membrane

(A) Microsomal membranes from HEK293FT cells expressing pcDNA, Hhat WT, or Hhat H379A were incubated with [¹²⁵I] IodoPalmitoyl-CoA for 60 min at room temperature prior to the addition of 2% BSA. ¹²⁵I cpm remaining inside the vesicles after washing was quantified; n = 2.

(B) Microsomal membranes were pretreated for 15 min with 10 μM TDI-3410, then analyzed for [¹²⁵I] IodoPalmitoyl-CoA uptake; n = 3.

(C and D) Microsomal membranes containing WT Hhat were pretreated for 15 min with the indicated concentrations of TDI-3410.

(C) The amount of NBD-palmitoyl-CoA remaining within the vesicle was quantified; n = 3; IC₅₀ = 0.5 μM.

(D) Membranes were assayed for Shh palmitoylation activity by incubation with biotinylated Shh peptide and [¹²⁵I] IodoPalmitoyl-CoA; n = 2; IC₅₀ = 1.4 μM.

(E and F) Microsomal membranes from HEK293FT cells expressing Hhat or Porcupine were pretreated for 15 min with (E) 5 μM malonyl-CoA, (F) 10 μM TDI-3410, 10 μM Etomoxir, or both TDI-3410 and Etomoxir. NBD-palmitoyl-CoA uptake was determined (n = 3) as in Figure 1.

(G) As in (F), but with the gain on the plate reader increased; n = 3, *p = 0.03; **p = 0.003.

(H) Purified Hhat was incubated with 10 μM TDI-3410 or 10 μM Etomoxir, and Shh palmitoylation activity was assayed; n = 3.

See also Figure S1.

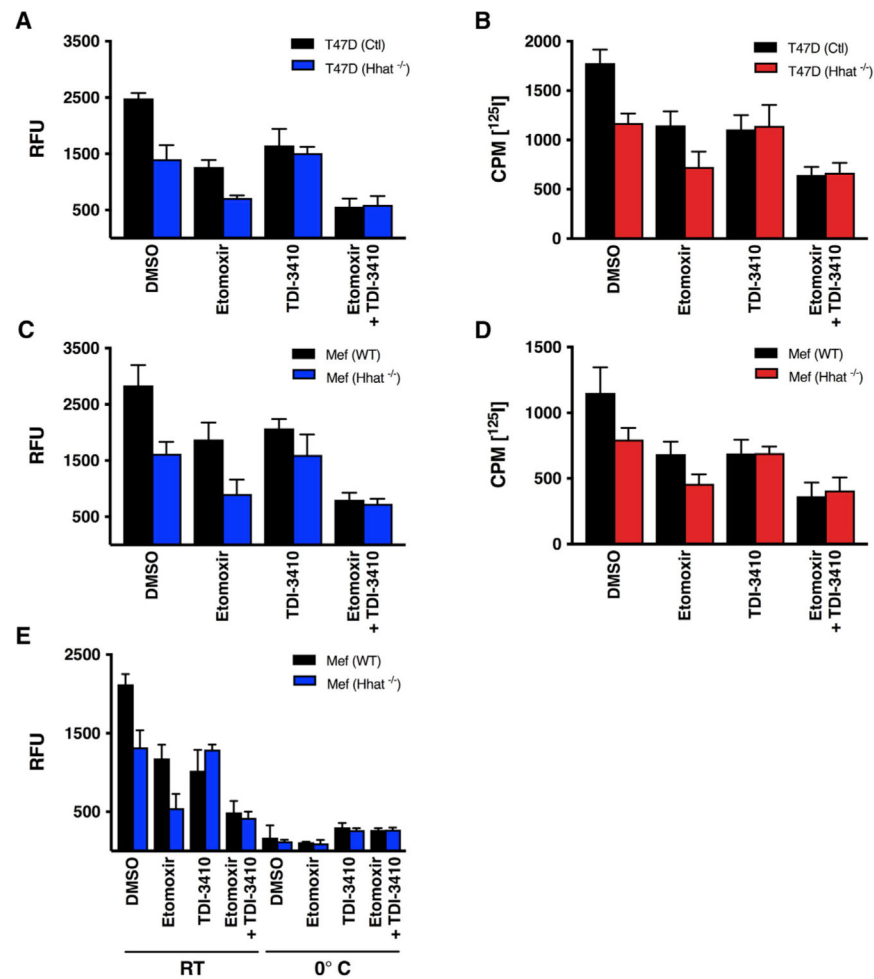


Figure 3. NBD-Palmitoyl-CoA Uptake Is Reduced in Membranes from Hhat^{-/-} Cells
 (A–D) Microsomal membranes from control or Hhat^{-/-} T47D cells (A and B) or Hhat^{-/-} MEFs (C and D) were pretreated for 15 min with 10 μM TDI-3410, 10 μM Etomoxir, or both drugs, and the uptake of NBD-palmitoyl-CoA (A and C) or [¹²⁵I] IodoPalmitoyl-CoA (B and D) was determined as described in Figure 2. (A) n = 4; (B) n = 2; (C) n = 3; and (D) n = 2.
 (E) Microsomal membranes from (C) were pretreated for 15 min with 10 μM TDI-3410, 10 μM Etomoxir, or both drugs, and the NBD-palmitoyl-CoA uptake assay was performed at room temperature or at 0°C; n = 3.

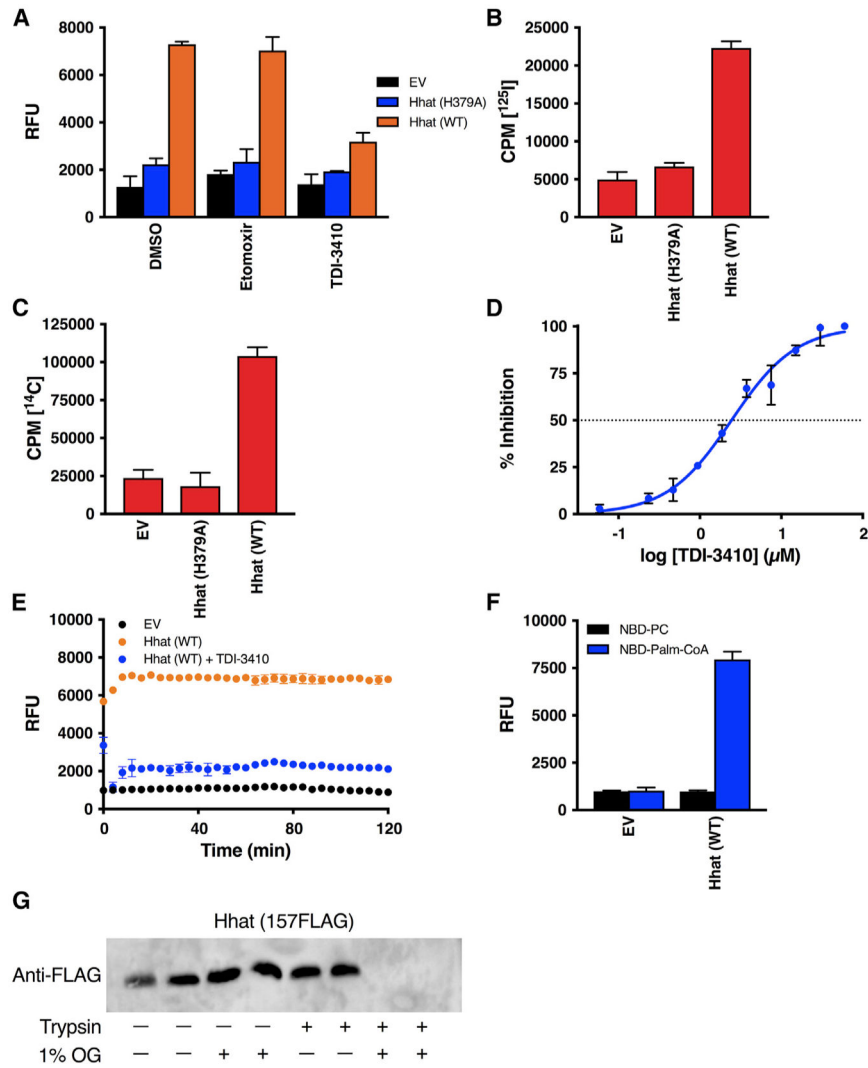


Figure 4. Purified Hhat Reconstituted into Artificial Liposomes Mediates Palmitoyl-CoA Uptake (A–C) The 0.2-μm liposomes reconstituted with or without purified Hhat WT or Hhat H379A were pretreated for 15 min with 10 μM TDI-3410 or 10 μM Etomoxir (A) and incubated for 60 min at room temperature with NBD-palmitoyl-CoA (A; n = 4), [¹²⁵I] IodoPalmitoyl-CoA (B; n = 2), or [¹⁴C] palmitoyl-CoA (C; n = 2), and palmitoyl-CoA uptake was determined as in Figures 1 and 2.

(D) Liposomes reconstituted with purified Hhat WT were pretreated with the indicated concentrations of TDI-3410 and NBD-palmitoyl-CoA uptake was analyzed as in (A); n = 3. (E) As in (A). After quencher addition, RFU readings were taken every 2 min for 120 min; n = 3.

(F) As in (A). Liposomes were incubated with either NBD-PC or NBD-palmitoyl-CoA; n = 2.

(G) Liposomes reconstituted with purified 157FLAG Hhat were treated with or without trypsin or octyl glucoside (OG), and Hhat was analyzed by SDS-PAGE and western blotting with anti-FLAG antibody.

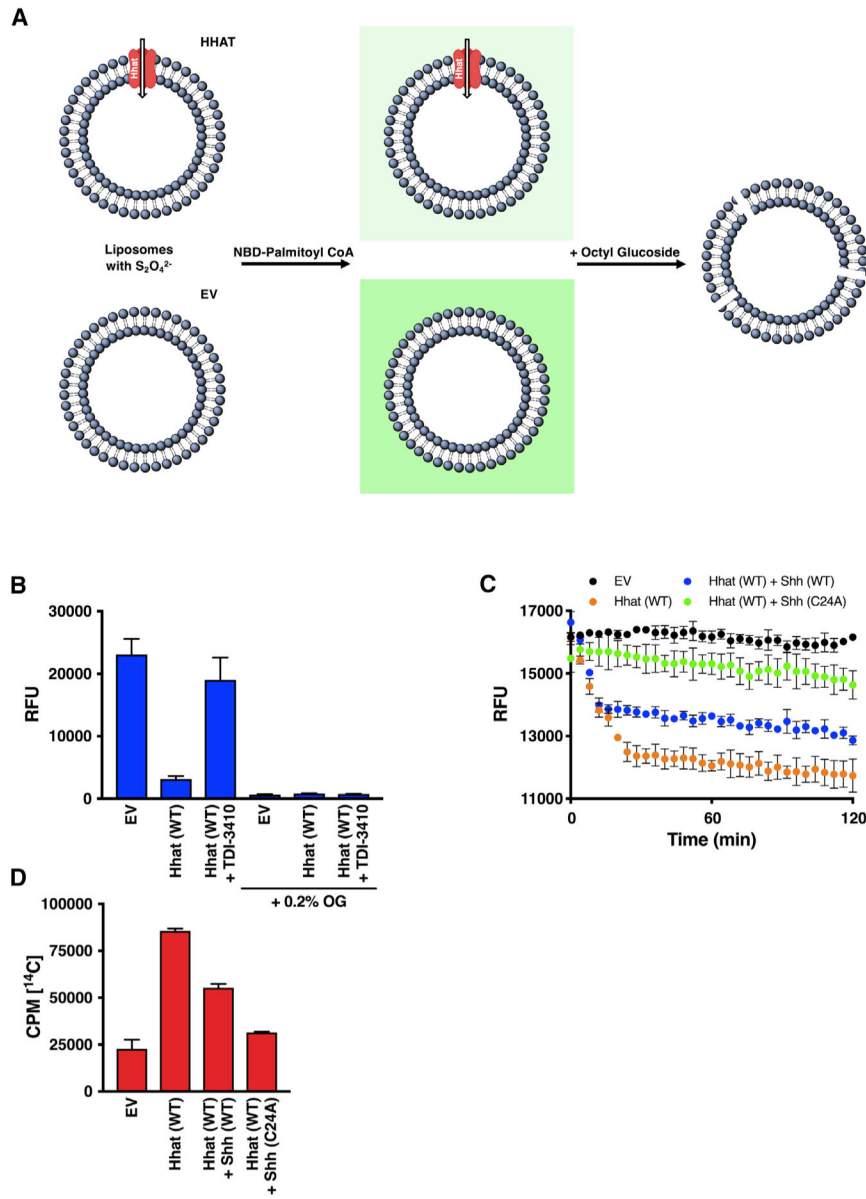


Figure 5. Quenching of Internalized NBD Fluorescence in Liposomes Containing Dithionite (A) Diagram of the modified NBD-palmitoyl-CoA uptake assay. Liposomes were reconstituted with or without purified Hhat (WT or H379A) in the presence of $\text{Na}_2\text{S}_2\text{O}_4^{2-}$. Liposomes were re-isolated and then incubated with NBD-palmitoyl-CoA, and NBD fluorescence was quantified. The addition of 0.2% octyl glucoside reduced fluorescence levels to background.

(B) Liposomes generated as in (A) were pretreated with 10 μM TDI-3410 for 15 min followed by incubation with NBD-palmitoyl-CoA for 60 min. RFU readings were taken before and after addition of 0.2% octyl glucoside; $n = 3$.

(C) Liposomes were reconstituted with purified WT Hhat, $\text{Na}_2\text{S}_2\text{O}_4^{2-}$, and WT or C24A Shh peptide. After the removal of the external quencher and peptide, NBD-palmitoyl-CoA was added, and the fluorescent signal was monitored for 120 min; $n = 3$.

(D) Liposomes were reconstituted with purified WT Hhat, and uptake of [¹⁴C] palmitoyl-CoA was measured as in Figure 4C; n = 2.

Author Manuscript

Author Manuscript

Author Manuscript

Author Manuscript

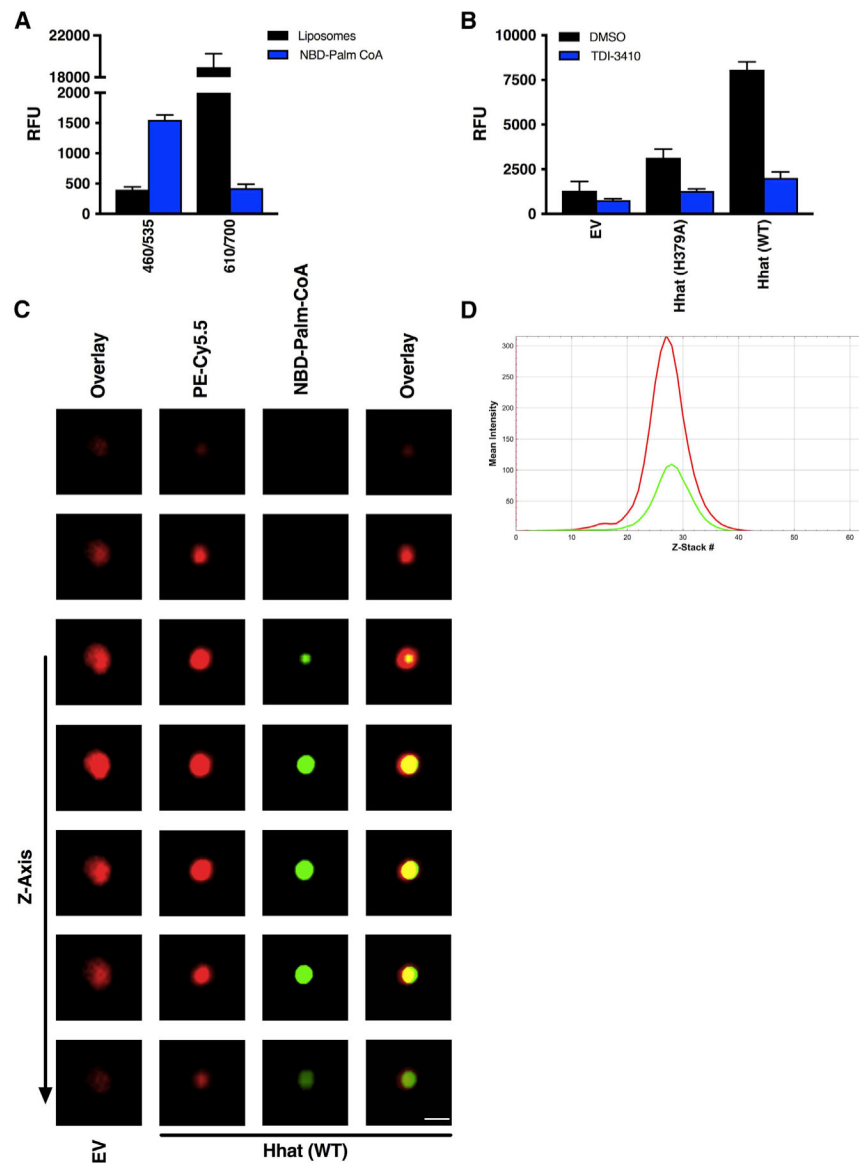


Figure 6. Visualization of Palmitoyl-CoA Uptake by Liposomes Containing Purified, Reconstituted Hhat

(A) RFU readings at 460/535 nm and 610/700 nm. Fluorescent intensity of liposomes containing Cy5.5-PE integrated into the membrane or NBD-palmitoyl-CoA alone at 460/535 nm and 610/700 nm was determined; $n = 3$. No signal inference between the signals for the Cy5.5 and NBD was observed.

(B and C) Membrane-integrated Cy5.5-PE liposomes reconstituted with or without purified Hhat (WT or H379A) were pretreated with 10 μM TDI-3410 for 15 min followed by incubation with NBD-palmitoyl-CoA for 60 min at room temperature prior to quenching with $\text{Na}_2\text{S}_2\text{O}_4^{2-}$.

(B) RFU readings; $n = 3$.

(C) Images of liposomes containing membrane integrated PE (red: Cy5.5-PE) and palmitoyl-CoA (green: NBD-palmitoyl-CoA) were acquired by confocal microscopy. Scale bar, 0.2 μm .

(D) Line scan of fluorescence intensities of Z stacks from Video S1.

Author Manuscript

Author Manuscript

Author Manuscript

Author Manuscript

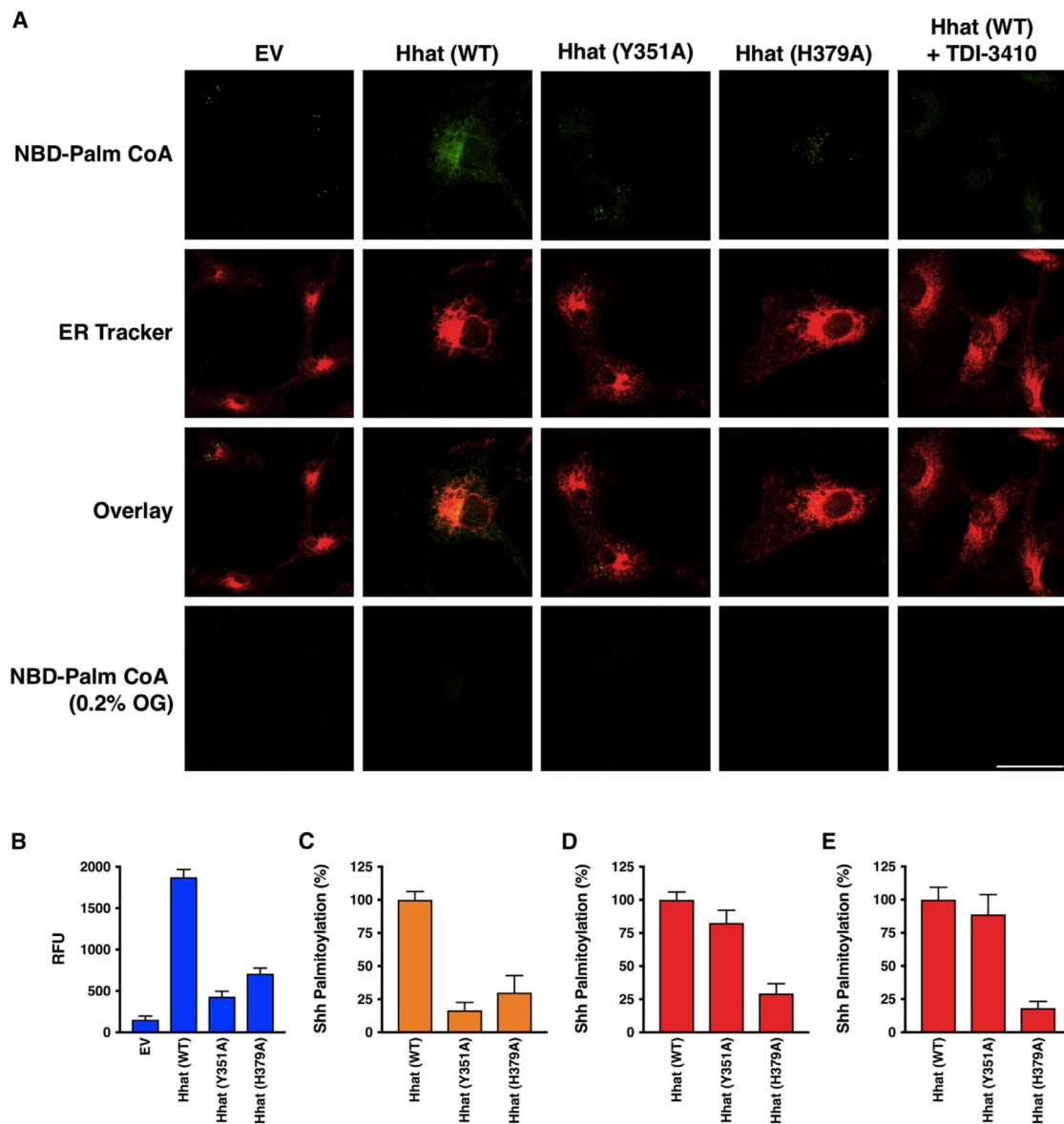


Figure 7. Palmitoyl-CoA Uptake and Shh Palmitoylation in Cells Expressing Hhat

(A) COS-7 cells expressing EV, Hhat WT, Hhat H379A, or Hhat Y351A were incubated on ice with 65 μ g/ml digitonin for 10 min to permeabilize the plasma membrane, then incubated for 60 min at room temperature with 8 μ M NBD-palmitoyl-CoA. 30 min prior to imaging, 1 μ M ER Tracker Red was added to the cells. Cells were washed and then imaged by confocal microscopy. Scale bar, 25 μ m.

(B) NBD-palmitoyl-CoA uptake was monitored in microsomal membranes from HEK293FT cells expressing EV, Hhat WT, Hhat H379A, or Hhat Y351A as described in Figure 2; n = 3.

(C) Shh palmitoylation was monitored in COS-1 cells expressing Shh and either pcDNA, WT, or mutant (H379A, Y351A) Hhat. Cells were incubated with 15 μ Ci [125 I] IodoPalmitate for 4 h, lysed, and Shh immunoprecipitated from cell lysates was analyzed by SDS-PAGE. [125 I] CPM incorporated into Shh was quantified by phosphorimaging; n = 2.

(D) Shh palmitoylation was monitored in microsomal membranes from (B). Membranes were incubated with biotinylated Shh peptide and [125 I] IodoPalmitoyl-CoA for 60 min prior to the addition of streptavidin-agarose beads. Beads were washed, and [125 I] CPM incorporated into the Shh peptide were determined in a gamma counter; n = 2. See also Figure S2.

(E) Shh palmitoylation activity was assayed using purified Hhat as in (D); n = 2.

KEY RESOURCES TABLE

REAGENT or RESOURCE	SOURCE	IDENTIFIER
Antibodies		
Mouse monoclonal Flag-specific (anti-Flag) M2	Sigma-Aldrich	Cat # F3165; RRID:AB_259529
Rabbit polyclonal anti-HA	Sigma-Aldrich	Cat # H6908; RRID:AB_260070
Anti-Shh antibody (E-1)	Santa Cruz Biotechnology	Cat # sc-365112; RRID:AB_10709580
Anti-Shh antibody (G-5)	Santa Cruz Biotechnology	Cat # sc-373779; RRID:AB_10947241
Chemicals, Peptides, and Recombinant Proteins		
ProLong Glass Antifade Mountant	Fisher Scientific	P32980
ER-Tracker Red (BODIPY TR Glibenclamide)	Fisher Scientific	E34250
Triton X-100	Fisher Scientific	BP151
Sodium dithionite	Sigma-Aldrich	157953
Digitonin	Sigma-Aldrich	D6628
3 × Flag peptide	Sigma-Aldrich	F4799
Octyl glucoside	EMD Millipore	494459
[¹²⁵ I]NaI	PerkinElmer Life Sciences	NEZ033A
[¹⁴ C]-palmitoyl Coenzyme A	PerkinElmer Life Sciences	NEC555
{N-[(7-nitro-2-1,3-benzoxadiazol-4-yl)- methyl]amino} palmitoyl Coenzyme A (ammonium salt)	Avanti Polar Lipids	810705P
{N-[(7-nitro-2-1,3-benzoxadiazol-4-yl)- methyl]amino} phosphatidylcholine	Avanti Polar Lipids	810130P
1-palmitoyl-2-oleoyl-sn-glycero-3-phosphoethanolamine	Avanti Polar Lipids	850757P
L-α-phosphatidylcholine (Egg, Chicken)	Avanti Polar Lipids	840051P
1-palmitoyl-2-oleoyl-sn-glycero-3- phospho-L-serine (sodium salt)	Avanti Polar Lipids	840034P
Cy5.5 PE (1,2-distearoyl-sn-glycero-3-phosphoethanolamine-N-(Cyanine 5.5))	Avanti Polar Lipids	810346C
L-α-phosphatidylinositol (Liver, Bovine) (sodium salt)	Avanti Polar Lipids	840042P
Polybrene ®	Santa Cruz Biotechnology	sc-134220
GlutaMAX	GIBCO	35050061
Lipofectamine 2000	ThermoFisher	11668019
Critical Commercial Assays		
EZQuant Cell Quantifying Kit	ALSTEM	CQ01
QuikChange II XL Site directed mutagenesis kit	Stratagene	200521
TDI-3410	Tri-Institutional Therapeutics Discovery Institute	WO/2017/218874
Shh peptide (WT) CGPGRGFGKR-PEG2- K(Biotin)-NH ₂	AnaSpec	Custom synthesis
Shh peptide (C24A) AGPGRGFGKR-PEG2- K(Biotin)-NH ₂	AnaSpec	Custom synthesis
Experimental Models: Cell Lines		
COS-1	ATCC	ATCC CRL-1650
COS-7	ATCC	ATCC CRL-1651
HHAT -/- MEFs	Dr. Pao-Tien Chuang, UCSF	N/A

REAGENT or RESOURCE	SOURCE	IDENTIFIER
T47D	ATCC	ATCC HTB-133
HHAT --/ T47D	OriGene	CRISPR Kit# KN208447
HEK293FT	Invitrogen	R70007
Recombinant DNA		
HA-Hhat	Buglino and Resh, 2008	JBC 283:22076–88
HA-His-Flag Hhat	Buglino and Resh, 2008	JBC 283:22076–88
Software and Algorithms		
GraphPad Prism v8	GraphPad Software	https://www.graphpad.com
Imaris	Bitplane	https://imaris.oxinst.com.com/
Adobe Photoshop	Adobe Systems	https://www.adobe.com/products/photoshop.html
Fiji (ImageJ)	Open-source	https://fiji.sc/#download
Other		
Black Polystyrene Microplates	Fisher Scientific	07-200-565
Sephadex® G-75	Sigma-Aldrich	GE17–0051-01
FlagM2 agarose	Sigma-Aldrich	A2220
μ -Slide Angiogenesis	ibidi	81506
Nunc® Lab-Tek® II chambered coverglass	MSKCC Molecular Histology Core	N/A